

Reggeon field theory with a threshold approach to secondary Reggeons

A. García

Centro Atómico Bariloche and Instituto de Física Balseiro, Comisión Nacional de Energía Atómica and Universidad Nacional de Cuyo, Bariloche, Argentina

C. A. García Canal

Departamento de Física, Universidad Nacional de La Plata, La Plata, Argentina

N. Parga

Centro Atómico Bariloche and Instituto de Física Balseiro, Comisión Nacional de Energía Atómica and Universidad Nacional de Cuyo, Bariloche, Argentina

(Received 13 October 1977)

A Reggeon-field-theory model is proposed for secondary Reggeons interacting with a Pomeron which has a rapidity threshold related to the onset of diffractive effects. Under the assumption of a critical Pomeron, a solution is found with the aid of renormalization-group techniques and the model is successfully tested against the experimental $\pi^{\pm}p$ total-cross-section difference.

I. INTRODUCTION

Reggeon field theory (RFT) tells us how to deal with t -channel unitarity corrections to the Pomeron¹ and to secondary Reggeons.² However, some of these corrections turn out to be divergent and therefore any phenomenological application requires the introduction of an unknown cutoff. Another difficulty of RFT appears when dealing with a critical Pomeron since in this case the intercept renormalization δ_p cannot be calculated perturbatively and the use of an integral representation must again be supplemented by the introduction of a cutoff.³

In the case of the Pomeron it is possible to regularize the theory in an alternative way realizing that this singularity needs a threshold in energy to manifest itself.⁴ This method has proved useful in predicting the pp total cross-section rise in the Fermilab and CERN ISR range without modifying the critical behavior of the Pomeron.⁵ Here a fundamental role is played by the nonperturbative δ_p which is simultaneously regularized by the introduction of the above-mentioned threshold.

In this paper we shall show that when this Pomeron with threshold is coupled with a secondary Reggeon the resulting RFT is also finite. At the same time this threshold will let us obtain a finite nonperturbative Reggeon-intercept renormalization and will provide, as in the Pomeron theory,⁴ a rule to select those diagrams which contribute at any given energy. This modified RFT defines therefore an alternative approach, giving a physical amplitude finite and exact at each energy, as opposed to the coupling-constant expansion of the usual RFT. This property, together with the fact that there is no need for an ϵ expansion,

makes our proposal a model of obvious phenomenological interest. It must be remarked that we are not assigning any threshold to the secondary Reggeon in accordance with the traditional arguments of duality. As we will argue later on, this implies that no flavoring effects are present for this singularity.

The techniques of the renormalization group will enable us to give closed integral expressions for the relevant quantities of the theory even though the existence of two coupling constants implies some technical difficulties.

To show how the model works, we analyze the ρ singularity in the total-cross-section difference $\Delta\sigma = \sigma_{\pi^-p} - \sigma_{\pi^+p}$. It is by now well known that a pure ρ Regge pole does not give an adequate description of πN charge-exchange (CEX) data not only because of polarization phenomena, but also for two other reasons⁶: (a) There is no simple compromise pole that simultaneously fits $\Delta\sigma$ and the rapid decrease of $d\sigma_{\text{CEX}}/dt|_{t=0}$ at high energy, and (b) $\Delta\sigma$ needs a greater effective ρ intercept at low energy than at higher energies. In the RFT we are proposing, the renormalized singularity behaves quite similarly to a simple pole, though it presents a decreasing effective intercept in agreement with experimental data. This decreasing behavior is a straightforward consequence of the positiveness of the Reggeon-intercept counterterm.

In Sec. II the RFT model is defined through its Feynman rules and the necessary integral representations are derived, whereas in Sec. III we make the approximations which allow us to find a consistent solution for them. We also give here the asymptotic behavior of the model amplitude which is of the same form as for the theory with-

out thresholds. We compare the prediction of the model with the ρ -exchange amplitude in πN scattering data in Sec. IV, and finally the conclusions are summarized in Sec. V.

II. THE RFT MODEL AND INTEGRAL REPRESENTATIONS

The RFT we propose describes the interaction of Pomerons and Reggeons with number conservation for the latter and autointeractions for the former in the spirit of AS (Ref. 2) but with a Pomeron with a threshold Δ in rapidity according to Ref. 4. The theory is defined by the Feynman rules listed in AS (whose notation and conventions we adopt) except for the Pomeron propagator that now reads

$$G_0^{(1,1;0)}(E, \vec{q}^2) = \frac{i \exp[i(E - \alpha'_0 \vec{q}^2)t_0]}{E - \alpha'_0 \vec{q}^2 + i\epsilon}, \quad (1)$$

where after any loop integration t_0 is meant to be Wick rotated to the physical value Δ , whereas we maintain the usual form for the Reggeon propagator

$$G_0^{(0,0;1)}(\mathcal{E}, \vec{p}^2) = \frac{i}{\mathcal{E} - \alpha'_R \vec{p}^2 + i\epsilon}, \quad (2)$$

with

$$\mathcal{E} = \alpha_R(0) - J \quad (3)$$

as obtained after a gauge transformation (AS). Since in our scheme Reggeons cannot be created or destroyed the Pomeron turns out to be the same as that of Ref. 5 and we need only study its influence on the Reggeon. One immediate consequence of this influence will be that each diagram has a rapidity threshold given by the rule of Ref. 4 with zero threshold for the Reggeon.

As an example of the way the theory is regularized we can easily calculate the second-order Reggeon self-energy (Fig. 1)

$$\begin{aligned} \Sigma^{(2)}(\mathcal{E}, \vec{p}^2) &= \frac{\lambda_0^2}{4\pi} \frac{1}{(\alpha'_0 + \alpha'_{R_0})} \\ &\times E_1 \left[- \left(\mathcal{E} - \frac{\alpha'_0 \alpha'_{R_0}}{\alpha'_0 + \alpha'_{R_0}} \vec{p}^2 \right) \Delta \right], \quad (4) \end{aligned}$$

which is now seen to be convergent (in two dimensions) owing to the presence of Δ . For finite Δ

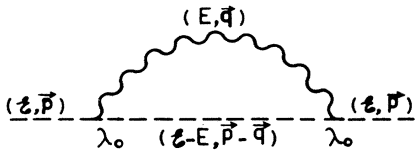


FIG. 1. Second-order contribution to the Reggeon self-energy.

it has a branching point at $\mathcal{E} = 0$ with the usual slope.

We start our renormalization-group analysis by stating the normalization conditions for the vertex parts which define δ_P and the renormalized quantities Z , α' , and r for the Pomeron⁴:

$$\Gamma^{(1,1;0)}(E, \vec{q}^2) \Big|_{\substack{\mathcal{E}=0 \\ \vec{q}^2=0}} = 0, \quad (5a)$$

$$\frac{\partial}{\partial E} i\Gamma^{(1,1;0)}(E, \vec{q}^2) \Big|_{\substack{\mathcal{E}=-E_N \\ \vec{q}^2=0}} = (1 + \Delta_N) e^{\Delta_N}, \quad (5b)$$

$$\frac{\partial}{\partial \vec{q}^2} i\Gamma^{(1,1;0)}(E, \vec{q}^2) \Big|_{\substack{\mathcal{E}=-E_N \\ \vec{q}^2=0}} = -\alpha'(E_N)(1 + \Delta_N) e^{\Delta_N}, \quad (5c)$$

$$\Gamma^{(1,2;0)}(E_1, \vec{q}_1^2, \dots, E_3, \vec{q}_3^2) \Big|_{\substack{E_1=2E_2=2E_3=-E_N \\ \vec{q}_i=0}} = \frac{r(E_N)}{(2\pi)^{3/2}}, \quad (5d)$$

where $\Delta_N = \Delta E_N$. For the Reggeon ones, δ_R , Z_R , α'_R , and λ , the conditions quoted in AS are not modified.

From these last relations and following the steps of the Pomeron case,³ one immediately obtains for the Reggeon intercept counterterm

$$\delta_R = \Sigma(\mathcal{E}, \vec{p}^2) \Big|_{\substack{\mathcal{E}=0 \\ \vec{p}^2=0}} = \int_{-\infty}^0 \left(1 - \frac{1}{Z_R} \right) d(-E_N). \quad (6)$$

As for the Pomeron counterterm, this expression cannot be evaluated perturbatively as we shall explicitly see later on. We therefore seek a renormalization-group calculation for Z_R .

If β , γ , and ζ (β_R , γ_R , and σ) are the standard renormalization-group functions for the Pomeron (Reggeon) depending only on the dimensionless quantities g , g_R , ν , and Δ_N , it is straightforward to get the integral representation

$$Z_R(g, g_R, \nu, \Delta_N) = \exp \left[\int_{\bar{\mathcal{E}}(\bar{\mathcal{E}}_R=0)}^{\mathcal{E}} d\bar{g} \frac{\gamma_R(\bar{g}, \bar{g}_R, \bar{\nu}, \Delta_N)}{\beta(\bar{g}, \Delta_N)} \right], \quad (7)$$

where the dependence of g in E_N is given by

$$g^2 = g_0^2 / (1 + g_0^2/g_1^2),$$

with $g_0^2 = r_0^2 / (\alpha'_0 E_N)$ and g_1 , the zero of β , is the function of Δ_N given in Ref. 5. On the other hand, the g_R dependence on E_N is obtained from the integral representation

$$Z_{\bar{g}_R}(g, g_R, \nu, \Delta_N) = g_R(E_N)/g_{R_0} = Z_{\bar{g}_R}(0, \bar{g}_R(\bar{g}=0), \bar{\nu}(\bar{g}=0), \Delta_N) \exp\left[\int_0^{\bar{g}} d\bar{g} \left(\frac{1}{2} + \frac{\beta_R(\bar{g}, \bar{g}_R, \bar{\nu}, \Delta_N)}{\bar{g}_R}\right) \frac{1}{\beta(\bar{g}, \Delta_N)}\right], \quad (8)$$

with $g_{R_0}^2 = 2\lambda_0^2/[(\alpha'_0 + \alpha'_{R_0})E_N]$, where \bar{g}_R and $\bar{\nu}$ are the solutions to the coupled differential equations

$$\frac{d\bar{g}_R}{d\bar{g}} = \frac{\beta_R(\bar{g}, \bar{g}_R, \bar{\nu}, \Delta_N)}{\beta(\bar{g}, \Delta_N)} \quad (9a)$$

and

$$\frac{d\bar{\nu}}{d\bar{g}} = \frac{\sigma(\bar{g}, \bar{g}_R, \bar{\nu}, \Delta_N)}{\beta(\bar{g}, \Delta_N)}, \quad (9b)$$

with the boundary conditions

$$\left. \begin{array}{l} \bar{g}_R = g_R \\ \bar{\nu} = \nu \end{array} \right\} \text{ for } \bar{g} = g. \quad (10)$$

In principle one needs an equivalent expression for $\nu = \nu(E_N)$. However, we shall in a short while give arguments for leaving ν aside.

III. A SOLUTION TO THE RENORMALIZATION-GROUP EQUATIONS

In the preceding section we set up the integral representations for δ_R and the other relevant quan-

ties. To proceed further we calculate the Reggeon renormalization-group functions

$$\gamma_R(g, g_R, \nu, \Delta_N) = E_N \frac{\partial \ln Z_R}{\partial E_N} \Big|_{r_0, \lambda_0, \alpha'_0, \alpha'_{R_0}, \Delta_N}, \quad (11a)$$

$$\beta_R(g, g_R, \nu, \Delta_N) = E_N \frac{\partial g_R}{\partial E_N} \Big|_{r_0, \lambda_0, \alpha'_0, \alpha'_{R_0}, \Delta_N}, \quad (11b)$$

$$\sigma(g, g_R, \nu, \Delta_N) = E_N \frac{\partial \nu}{\partial E_N} \Big|_{r_0, \lambda_0, \alpha'_0, \alpha'_{R_0}, \Delta_N}, \quad (11c)$$

by solving perturbatively Eqs. (5) for Z_R , g_R , and ν . To second order

$$\gamma_R = -\frac{g_R^2}{8\pi} e^{-\Delta_N}, \quad (12a)$$

$$\beta_R = -g_R(\frac{1}{2} + C_1 g^2 + C_2 g g_R + C_3 g_R^2), \quad (12b)$$

$$\sigma = -\frac{1}{8\pi} \frac{\nu}{1+\nu} \left[g_R^2 \nu e^{-\Delta_N} - \frac{g^2}{4} (1+\nu) \frac{e^{-2\Delta_N}}{1+\Delta_N} \right], \quad (12c)$$

where

$$C_1 = \frac{1}{64\pi} \frac{e^{-2\Delta_N}}{1+\Delta_N} \frac{1+2\nu}{1+\nu},$$

$$C_2 = \frac{1}{2\pi} \frac{1}{[2(1+\nu)]^{1/2}} \left\{ \frac{1+\nu}{3-\nu} \left[\exp\left(\frac{3-\nu}{1+\nu} \frac{\Delta_N}{2}\right) E_1\left(\frac{2\Delta_N}{1+\nu}\right) - E_1\left(\frac{\Delta_N}{2}\right) \right] + e^{\Delta_N/2} E_1(2\Delta_N) - e^{-\Delta_N/2} E_1(\Delta_N) \right\}, \quad (13)$$

$$C_3 = \frac{1}{4\pi} \left\{ \frac{e^{-\Delta_N}}{4} \left[2 - \frac{\nu^2}{(1+\nu)^2} \right] + E_1(\Delta_N) - E_1\left(\frac{\Delta_N}{2}\right) \right\}.$$

The critical points correspond to the simultaneous zeros of β , β_R , and σ . It is easily checked that an infrared-stable zero is obtained for the positive root, g_{R_1} , of Eq. (12b), $\nu = \nu_1 = 0$, and of course the zero of β .

In order to simplify Eqs. (9) we assume that the solution for $\bar{\nu}$ does not depart too much from its critical value $\nu_1 = 0$. Since for this ν value σ vanishes, Eq. (9b) is satisfied. (Note that this equation would not even appear if slope renormalizations were not taken into account.) To make the remaining Eq. (9a) easily solvable, we note that a numerical evaluation of Eqs. (13) gives a C_3 value much smaller than gC_2 and $(\frac{1}{2} + g^2 C_1)$ in the range of interesting E_N values and we can there-

fore neglect its contribution to β_R . Within these approximations, the solution to Eq. (9a) is readily found to be

$$\bar{g}_R = \bar{g} \left[\frac{g_1}{g_{R_1}} + \left(\frac{g}{g_R} - \frac{g_1}{g_{R_1}} \right) \left(\frac{g_1^2 - \bar{g}^2}{g_1^2 - g^2} \right)^{1/2 + C_1 g_1^2} \right]^{-1}, \quad (14)$$

which verifies the initial condition, Eq. (10), and goes through the critical point $\bar{g}_R(g_1) = g_{R_1}$ where now the zero of β_R simplifies to

$$g_{R_1} = (\frac{1}{2} + C_1 g_1^2) / (C_2 g_1). \quad (15)$$

With these values of $\bar{\nu}$ and \bar{g}_R we obtain finally

$$Z_R(g, g_R, \nu, \Delta_N) = \left(\frac{y_1}{y_2} \frac{1+y_2}{1+y_1} \right)^{\gamma_{R_1}/(1/2+C_1 g_1^2)} \times \exp \left[\frac{y_2 - y_1}{(1+y_1)(1+y_2)} \frac{\gamma_{R_1}}{(1/2+C_1 g_1^2)} \right], \quad (16)$$

with

$$\gamma_{R_1} = \gamma_R(g_{R_1}),$$

$$y_1 = \frac{g g_{R_1}}{g_R g_1} - 1,$$

$$y_2 = y_1 (1 - g^2/g_1^2)^{-1/2 - C_1 g_1^2}.$$

As a check we remark that a series development of this expression in lowest order of g_R gives

$$Z_R \approx 1 + \frac{e^{-\Delta_N}}{8\pi} g_R^2, \quad (17)$$

which coincides with a direct perturbative calculation using Eq. (4). By the way, one sees that the corresponding perturbative calculation for δ_R is not allowed. In fact substituting Eq. (17) into Eq. (6), one gets

$$\delta_R = \lim_{\epsilon \rightarrow 0} G^2 E_1(\epsilon, \Delta), \quad (18)$$

with $G^2 = \lambda_0^2 / [4\pi(\alpha'_0 + \alpha'_{R_0})]$, which diverges. Note that since Δ acts as an ultraviolet cutoff, it cannot regularize this infrared divergence.

$$\Delta\sigma^{(2)}(Y) = \beta_\rho e^{-Y[1-\alpha_R(0)-\delta_R]} \left\{ 1 - G^2 \left[[E_1(\delta_R \Delta) - E_1(\delta_R Y)] Y + \frac{e^{-\delta_R Y} - e^{\delta_R \Delta}}{\delta_R} \right] \theta(Y - \Delta) \right\}, \quad (21)$$

and for $Y < \Delta$, the $\Delta\sigma$ behavior is governed by the bare pole $\alpha_{R_0} = \alpha_R(0) + \delta_R$. Note that near $Y \approx \Delta$, this expression simplifies into

$$\Delta\sigma^{(2)}(Y) \approx \beta_\rho e^{-Y[1-\alpha_R(0)-\delta_R]} \times \left[1 - G^2 \frac{e^{-\Delta\delta_R}}{\Delta} (Y - \Delta)^2 \theta(Y - \Delta) \right], \quad (22)$$

which gives a correction identical, except for the sign, to the old multicluster models result.⁸ As is well known, the minus sign here comes from the dominance of absorptive effects in RFT.⁹

We have chosen for the asymptotic Reggeon intercept the conventional values $\alpha_R(0) = 0.5$ and $\alpha'_0 = 0.3 \text{ GeV}^{-2}$ and $\alpha'_{R_0} = 1 \text{ GeV}^{-2}$ for the Pomeron and Reggeon slopes, respectively. The value of Δ is determined by the assumption that Pomeron effects appear at the same energy of the incoming

According to Ref. 4 one is quickly convinced that the amplitude's asymptotic behavior is of the form

$$A(s, 0) \sim s^{\alpha_R(0)} (\ln s)^{-\gamma_{R_1}},$$

as in AS, but now with $\gamma_{R_1} = -g_{R_1}^2/8\pi \approx -0.11$. [This number results from Eq. (15) with $g_1^2 = 5.86$ as in Ref. 5 and the remaining parameters in the infrared limit $\nu_1 = 0$, $\Delta_N = 0$.]

IV. A TEST OF THE MODEL

To find out how sensible the model is from a phenomenological viewpoint we shall compare it with experimental πN data. In order to do this, we assume that the full partial-wave amplitude is well approximated by the two-point Reggeon Green's function⁷ (an asymptotically valid statement), and therefore the total cross-section difference is given by

$$\Delta\sigma(Y) = \frac{\beta_\rho}{2\pi i} \int_{c-i\infty}^{c+i\infty} d(-E) \frac{i}{\Gamma^{(0,0;1)}(E, 0)} e^{-YE}, \quad (19)$$

where $Y = \ln(s/m\mu)$ with m (μ) the nucleon (pion) mass and β_ρ is the $\rho\pi N$ coupling. Here

$$i\Gamma^{(0,0;1)}(E, 0) = \mathcal{E} - \Sigma(\mathcal{E}, 0) + \delta_R, \quad (20)$$

where the nonperturbative δ_R is calculated using Eq. (6) and we take $\Sigma(\mathcal{E}, 0)$ from the second-order perturbative calculation, Eq. (4). We obtain

particles independent of the particular reaction. Taking into account the value adopted for $p p$ scattering⁵ $\Delta_p = 2.7$, we here have¹⁰ $\Delta = 2.7 + \ln(m/\mu) = 4.6$. This implies that Eq. (21) is exact up to $Y = 2\Delta$ or $p_{1ab} \approx 650 \text{ GeV}/c$. We also take from this last reference the same bare triple-Pomeron coupling r_0 .

The coupling G was determined in such a way that together with the δ_R resulting from Eq. (6), it gives good agreement with $\Delta\sigma$ experimental data all over the range $3.62 < p_{1ab} < 240 \text{ GeV}/c$. With¹¹ $G^2 \approx 0.06$ one gets $\delta_R \approx 0.05$ and the prediction of Fig. 2. As seen in this figure, this intercept renormalization provides a very adequate effective ρ -pole intercept to match the lower-energy data¹² while allowing the steep decrease necessary for the Fermilab region. In fact the effective intercept, given by

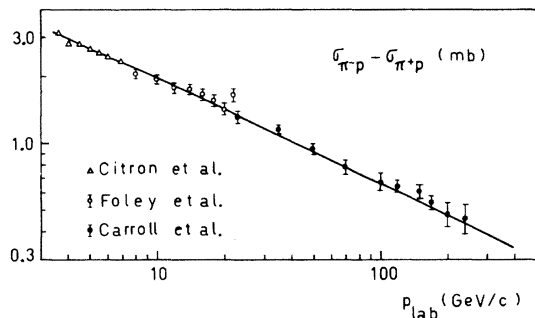


FIG. 2. Model prediction for $\Delta\sigma = \sigma_{\pi^-p} - \sigma_{\pi^+p}$ [Eq. (21)]. Data are from Ref. 12.

$$\alpha_{\text{eff}} = \alpha_{R_0} - \frac{\beta_\rho}{\Delta\sigma(Y)} G^2 e^{-Y(1-\alpha_{R_0})} \times [E_1(\delta_R \Delta) - E_1(\delta_R Y)] \theta(Y - \Delta), \quad (23)$$

decreases by ~ 0.03 in the experimental data range¹³ as seen in Fig. 3. However, the prediction of this model for $\Delta\sigma$ almost coincides with the simple pole at 0.48 of Ref. 14 from 20 up to 240 GeV/c, whereas our model and the simple pole appreciably differ below this energy where our model still provides very good agreement with data. Besides, the low-intercept behavior at high energy lets us foresee a satisfactory prediction for $d\sigma_{\text{CEX}}/dt|_{t=0}$, a long-standing problem in πN scattering.⁶

It is interesting to note again that we are able to reproduce $\Delta\sigma$ in the whole range $3.62 < p_{\text{lab}} < 240$ GeV/c with just one extra parameter G (the threshold value Δ is fixed by pp total-cross-section behavior⁵). Had we introduced pair-production thresholds or considered nonleading corrections in Eq. (19), we would have been faced with a wealth of new parameters. From our analysis this is apparently not required.

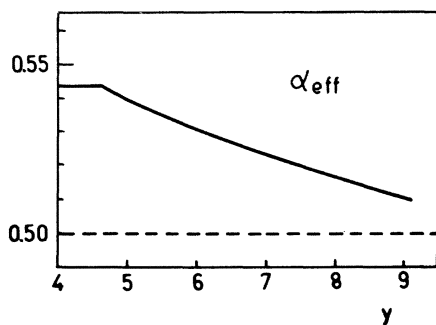


FIG. 3. The solid-line represents the ρ effective trajectory intercept as a function of rapidity [Eq. (23)]; the dashed line represents the asymptotic limiting value.

V. CONCLUSIONS

Within the framework of RFT we have discussed the coupling of a critical Pomeron with a secondary Reggeon when a threshold in rapidity is assigned to the former. Aided, as usual, by renormalization-group techniques we were able to find a consistent solution. Similar to what happens in the Pomeron sector, this threshold is enough to regularize the self-energy of the Reggeon, the only (ultraviolet) divergent quantity of the theory. Simultaneously it provides a threshold for each RFT diagram, thus allowing one to easily select those contributing to a fixed energy. Both facts are essential for making contact with experimental data below the transition energy, just where data are available, a property which is not evident in the usual RFT.

We have found that even though the Pomeron threshold eliminates the ultraviolet divergences of the theory, the surviving infrared ones did force us to make a nonperturbative evaluation of the Reggeon intercept counterterm. This fact played a very important role in explaining the decrease of the effective ρ intercept in πN from its low-energy value $[\alpha_R(0) + \delta_R]$ to the asymptotic limit $\alpha_R(0)$. It is worth noting that precisely the same Pomeron with threshold has been shown able to give the effective intercept needed to fit the pp total-cross-section data.⁵ There are, however, some points to comment on in this connection. In pp the Pomeron threshold produces⁵ a rising term $\delta_P(Y - 2\Delta_P)\theta(Y - 2\Delta_P)$ and the one-loop correction does not enter until $3\Delta_P$, i.e., above the experimental data points. For ρ instead, there is no rising term and the first correction comes from the loop and starts at $Y = \Delta$, well inside the experimental range available. The absence of a linear term in δ_R is due to the fact that no threshold has been assigned to the Reggeon propagator, Eq. (2), a hypothesis supported by the duality argument that ρ behavior appears, at least on the average, at the lowest energies. If one sticks to the argument of Ref. 15 in the sense that a term of this type should be associated to flavoring effects due to pair production, one concludes that effects of this kind are here unnecessary or negligible because of the above-mentioned duality hypothesis. In fact an intent of building a flavored¹⁶ ρ has been proved¹⁷ to be inconsistent with $d\sigma_{\text{CEX}}/dt|_{t=0}$ data unless a fairly large absorption is introduced by hand resulting in a very different effective intercept behavior.

Summarizing, an RFT model for secondary Reggeons has been solved which explains the non-Regge features of currently available data on the π^*p total cross-section difference. This was

achieved through the introduction of a rapidity threshold for the onset of Pomeron behavior while the results have required none for the secondary Reggeon. The loop correction then turns out at much lower energy than that required in the Pomeron case, and consequently secondary Reggeons seem to provide a better test ground for loop effects at present machine energies. In particular, we have seen that this correction is responsible for the observed decrease of the ρ effective inter-

cept in πN scattering.

ACKNOWLEDGMENT

We wish to warmly thank L. Masperi for invaluable comments and criticisms. Two of us (C.A.G.C.) and (N.P.) would like to thank the Consejo Nacional de Investigaciones Científicas y Técnicas, Argentina, for financial support.

¹H. D. I. Abarbanel, J. B. Bronzan, R. L. Sugar, and A. R. White, Phys. Rep. 21C, 119 (1975); M. Moshe, *ibid.* 37E, 257 (1978).

²H. D. I. Abarbanel and R. L. Sugar, Phys. Rev. D 10, 721 (1974). This will be referred to as AS.

³R. L. Sugar and A. R. White, Phys. Rev. D 10, 4074 (1974).

⁴A. Della Selva, A. García, C. A. García Canal, L. Masperi, and N. Parga, Phys. Lett. 62B, 311 (1976).

⁵A. García, C. A. García Canal, and L. Masperi, Phys. Lett. 66B, 442 (1977).

⁶A. Bouquet and B. Diu, Nuovo Cimento 29A, 373 (1975); A. García, C. A. García Canal, L. Masperi, and N. Parga, *ibid.* 32A, 1 (1976); H. Nakata, Phys. Rev. D 15, 927 (1977).

⁷To be rigorous, at non asymptotic energies one should include all Green's functions with diagrams contributing according to the rules of Ref. 4. In particular, for $\Delta < Y < 2\Delta$ one should consider a Y diagram for $\Gamma^{(0,1;1)}$ and another for $\Gamma^{(1,0;1)}$.

⁸W. R. Frazer, D. R. Snider, and Chung-I Tan, Phys. Rev. D 8, 3180 (1973); A. García, L. Masperi, and N. Parga, Nuovo Cimento 25A, 377 (1975).

⁹V. A. Abramovskii, V. N. Gribov, and O. V. Kanchelli,

Yad. Fiz. 18, 595 (1973) [Sov. J. Nucl. Phys. 18, 308 (1974)].

¹⁰This value may seem too high to fit $\{\sigma_{\pi-p} + \sigma_{\pi+p}\}$ data. However, this is not certain since in this channel other effects, e.g., secondary-trajectories contributions and Reggeon corrections to the Pomeron propagator, should complicate the simple analyses (Ref. 5) of the vacuum channel in pp .

¹¹A greater value was proposed in Ref. 17 to compensate increasing particle-production-thresholds contributions.

¹²A. Citron *et al.*, Phys. Rev. 144, 1101 (1966); K. J. Foley *et al.*, Phys. Rev. Lett. 19, 330 (1967); A. S. Carroll *et al.*, Phys. Lett. 61B, 303 (1976).

¹³A similar effect is proposed, although with a fairly larger decrease, by C. Pajares, Phys. Lett. 69B, 101 (1977).

¹⁴A. V. Barnes *et al.*, Phys. Rev. Lett. 37, 76 (1976).

¹⁵J. W. Dash, S. T. Jones, and E. K. Manesis, Phys. Rev. D 18, 303 (1978).

¹⁶J. Finkelstein and J. Koplik, Phys. Rev. D 14, 1467 (1976).

¹⁷A. García, C. A. García Canal, and L. Masperi, Phys. Rev. D 17, 917 (1978).

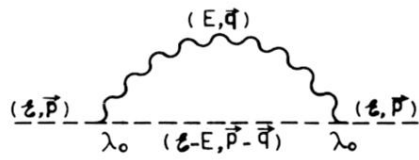


FIG. 1. Second-order contribution to the Reggion self-energy.

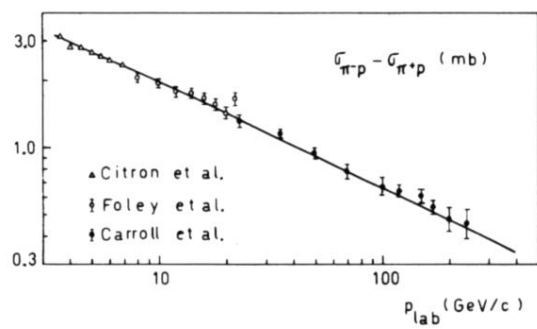


FIG. 2. Model prediction for $\Delta\sigma = \sigma_{\pi-p} - \sigma_{\pi+p}$ [Eq. (21)]. Data are from Ref. 12.

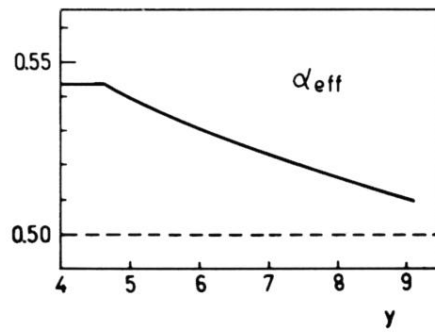


FIG. 3. The solid-line represents the ρ effective trajectory intercept as a function of rapidity [Eq. (23)]; the dashed line represents the asymptotic limiting value.